A Stochastic Geometry Approach to the Modeling of DSRC for Vehicular Safety Communication

Zhen Tong[1], *Student Member, IEEE,* Hongsheng Lu[2], Martin Haenggi[1], *Fellow, IEEE,* and Christian Poellabauer[2], *Senior Member, IEEE*

***Abstract*—Vehicle-to-vehicle safety communications based on the dedicated short range communication (DSRC) technology have the potential to enable a set of applications that help avoid traffic accidents. The performance of these applications, largely affected by the reliability of communication links, stringently ties back to the MAC and PHY layer design which has been standardized as IEEE 802.11p. The link reliabilities depend on the signal-to-interference-plus-noise ratio (SINR), which, in turn, depend on the locations and transmit powers of the transmitting nodes. Hence an accurate network model needs to take into account the network geometry. For such geometric models, however, there is a lack of mathematical understanding of the characteristics and performance of IEEE 802.11p. Important questions such as the scalability performance of IEEE 802.11p have to be answered by simulations, which can be very time-consuming and provide limited insights to future protocol design. In this paper, we investigate the performance of IEEE 802.11p by proposing a novel mathematical model based on queueing theory and stochastic geometry. In particular, we extend the Matern hard-core type II process with a discrete and non-uniform distribution, which is used to derive the temporal states of back-off counters. By doing so, concurrent transmissions from nodes within the carrier sensing ranges of each other are taken into account, leading to a more accurate approximation to real network dynamics. A comparison with ns2 simulations shows that our model achieves a good approximation in networks with different densities.**

***Index Terms*—IEEE 802.11p, Vehicular Ad Hoc Networks, Queueing Theory, Poisson Point Process, Matern Hard-core Point Process**

I. Introduction

A. Motivation

Vehicle-to-vehicle (V2V) safety communications based on DSRC at 5.9 GHz shows promising potential to improve driving safety on the road. With DSRC, every node (*i.e.*, vehicle) broadcasts up to 10 safety-related messages every second, where each message contains GPS information (*i.e.*, a vehicle's location, speed, and heading). Vehicles that receive such messages are able to track the senders, which therefore helps avoid vehicular collisions. At the lower layers, IEEE 802.11p provides the media access control and physical layer solution. However, prior studies have shown that IEEE 802.11p suffers a significant performance degradation when the number of nodes increases. It means a plunging delivery ratio of safety-related messages to recipients, leading to deteriorated tracking accuracy.

Many efforts have focused on improving the performance of IEEE 802.11p, most of which are based on simulations [1], [2]. However, it is extremely time-consuming, if not impossible, to simulate every case or combination of system parameters. A mathematical understanding is needed, to help save computational cost, to determine the fundamental performance limits and to provide guidance on the design of novel solutions. The performance depends critically on the signal-to-interference-plus-noise ratios (SINRs) at the receivers, and the signal strength and interference powers are functions of the distances between the nodes [3]. Realistic values for the internode distances and hence SINR values are obtained from geometric network models where nodes are placed on a line or one the plane according to some random process.

Our goal in this paper is to devise such geometric models that can accurately capture the temporal and spatial behavior of this CSMA-based protocol for different network configurations. We use both stochastic geometry and queueing theory for modeling and analysis of IEEE 802.11p. The model is exploited to predict the system performance in a more efficient manner than Network Simulator 2 (ns2) and to better understand the characteristics of IEEE 802.11p in V2V safety communications.

B. Related Work

A rich body of literature on the performance analysis of CSMA-based networks can be found in the research community, among which most works are based on queueing theory. For example, the performance of the carrier-sense multiple access with collision avoidance (CSMA/CA) scheme has been analyzed in [4], [5] using a discrete Markov chain model. The authors focused on one-hop networks (where all the nodes are within each other's carrier sensing range). A closed-form expression of the network throughput was developed with an assumption of saturated data traffic. Later, researchers applied the Markov chain approach to a broader set of cases. [6] investigated the impact of non-ideal channels and capturing techniques on the throughput of the IEEE 802.11 protocol with non-saturated data traffic. States for the transmission failures and states representing the case where no packets exist in the buffer are added into the model used in [4]. The throughput as a function of several parameters, such as packet size, is calculated. Authors in [7] characterized the impact of different

[1]Zhen Tong and Martin Haenggi are with the Department of Electrical Engineering, University of Notre Dame, Notre Dame, IN 46556, USA, E-mail: {ztong1,mhaenggi}@nd.edu.

[2]Hongsheng Lu and Christian Poellabauer are with the Department of Computer Science and Engineering, University of Notre Dame, Notre Dame, IN 46556, USA, E-mail: {hlu,cpoellab}@nd.edu.

message generation rates and transmission power levels on the network capacity in presence of of hidden terminals. Under some simplifying assumptions, the paper analyzed the hidden nodes and showed that the channel occupancy or busy ratio can be used as a feedback measure that quantifies the success of information dissemination. The work presented in [8] focuses on developing an accurate model for characterizing the impact of hidden terminals on the network performance. The authors pointed out the limitations of using renewal theory with a variable time slot in the literature and proposed a new model with a fixed-length channel slot. With a simple network topology, the model developed shows a good match with the simulations. In [9], [10], the authors investigated the performance of IEEE 802.11p with enhanced distributed channel access capability where applications with different priorities are divided into four access categories (ACs) according to their criticalities for the vehicle's safety. Since each AC has a separate back-off process, a AC can be viewed as a "virtual" node. Each virtual node competes with other virtual nodes as well as real nodes to get access to channel. The authors assumed that all the nodes observe the same channel to compute the throughput and delay using queueing theory, which constitutes an extension of [4], [5]. However, all the resulting models were either more complicated or only applicable to simplified network topologies.

On the other hand, stochastic geometry, in particular point process theory, has been widely used in the last decade to provide models and methods to analyze wireless networks, see [11]–[15] and references therein. Stochastic geometry provides a natural way of defining and computing critical performance metrics of the networks, such as the interference distribution, outage probability and so forth, by taking into account all potential geometrical patterns for the nodes, in the same way queueing theory provides response times or congestion, considering all potential arrival patterns.

To our best knowledge, the first paper using stochastic geometry to model the reliability of IEEE 802.11p protocol is [16]. However, it is limited to the analysis of dense vehicular networks using ALOHA to approximate the CSMA-based MAC protocol. Similarly, [17], [18] only focus on the performance analysis of vehicular networks using ALOHA as the MAC scheme. The connectivity of the vehicular networks in urban environments has been studied in [19]. A model based on stochastic geometry has been developed to obtain the probability of a node to be connected to the origin and the mean number of connected nodes for a given set of system parameters. However, the model does not explicitly take into account the temporal dynamics specific to vehicular networks, which are caused by factors like periodic traffic and the back-off process in IEEE 802.11p. The Matern hard-core process of type II [13, Chapter 3][3] has been used in [20] to analyze dense IEEE 802.11 networks, in which the nodes' locations are placed according to a Poisson point process and the random back-off counter is modeled as an independent mark that is associated with each node. However, the mark is assumed to be uniform between $[0, 1]$ which is not the case for IEEE 802.11p since the back-off counter takes only integer values from 0 to W, where W is the maximal value of the back-off counter (a typical value for W is 15).

[3]Starting with a basic uniform Poisson point process (PPP) Φ_b with intensity λ_b, add to each point x an independent random variable $m(x)$, called a mark, uniformly distributed in $[0, 1]$. All points that have a neighbor within distance r with a smaller mark are flagged. The remaining (non-flagged) points form the Matern hard-core process of type II.

C. Contributions

Our main contributions are:

1) We investigate the transmission behavior of V2V safety communications with non-saturated data traffic using a continuous-time Markov chain model that is based on a novel combination of queueing theory and point process theory. We show that the location distribution of the transmitting nodes is well modeled ranging from hard-core processes to PPPs as the network density increases, in contrast to [16], where only the dense case is studied.
2) A novel Matern hard-core process is proposed to capture the hard-core effect of CSMA and concurrent transmissions occurring within the same carrier sensing range. In particular, a modified Matern hard-core process of type II (called Matern-II-discrete process for the rest of the paper, whereas the original Matern hard-core process of type II [20] is henceforth called Matern-II-continuous process) is used with a discrete and non-uniform mark distribution to model the temporal information of the back-off counter and the spatial locations of the transmitting nodes. In this way, nodes with the same back-off counter value can transmit at the same time with nonzero probability even if they are within the carrier sensing range of each other, which makes the model more realistic.
3) We validate the effectiveness of our model by comparing it to other mathematical models and simulations from ns2, which have been calibrated for vehicle-to-vehicle communications by [1], [21] and will be used to generate ground truth in this study. The comparisons show that our model can be applied to networks of different densities with good accuracy.

D. Organization

The rest of the paper is organized as follows: Section II introduces the system model. In Section III, queueing theory and stochastic geometry are used to investigate the distribution of the transmitting nodes and the back-off counter distribution in networks with different densities. Section IV proposes and describes the Matern-II-discrete process in detail. The system performance is evaluated and compared with other models in Section V. We conclude our work in Section VI.

II. System Model

A. Traffic Model

We focus on V2V safety communications using DSRC at 5.9 GHz in the highway scenario where the transmission ranges of the vehicles are larger than the width of the road. Therefore, all the nodes can be assumed to be placed on a line according to a PPP with intensity λ_0. This set of nodes is denoted as Φ. Each node generates 10 messages every second as suggested in [22], which is equivalent to the requirement to transmit a message every 100 ms. These messages go to the same access category (AC), and traffic in other ACs [23] is out of the scope of this paper.

A message is dropped if it has not been sent out before a new one arrives. Since the message is beneficial to all nearby vehicles, broadcast communication is used, which means no RTS-CTS is exchanged before transmissions and no ACK is transmitted after a transmission. More specifically, when a message is available at a node, if the channel is idle, the message is broadcast immediately. Otherwise, a back-off counter in $[W] \triangleq \{0, 1, \cdots, W\}$ is drawn uniformly at random. $W + 1$ is called the contention window size; it is fixed since no ACK feedback is used.

A node has to go through a back-off process if it cannot send the message immediately, i.e., if its back-off counter is set. The back-off process executes in a EDCA (Enhanced Distributed Channel Access) manner where the decrement of the back-off counter value happens at the beginning. As shown in Fig. 1, when the channel becomes idle, the node decreases its back-off counter value immediately by one. It keeps doing so afterwards each time a time interval δ elapses (δ is called the slot time), and it freezes the count-down when the channel becomes busy again. When the value of the back-off counter reaches zero, if the channel stays idle within the following δ time (*i.e.*, slot time), the node starts transmitting right after. Otherwise, the node waits and the transmission will occur immediately after the channel turns idle next time.

B. Notation

From the above description, one can see that nodes may stay in different states (e.g., transmitting, back-off, idle) at a given time. These states (equivalently, called marks in point processes) need to be carefully understood and noted because they affect the distribution of interference across the network, which contributes to the reliability of communications. Hence, we list key notations used for point processes in Table I.

C. Channel Model

The power received at location y from a node located at point x, denoted by $P(x, y)$, is given by

$$P(x, y) = P \cdot S_y^x \cdot l(x, y), \tag{1}$$

where

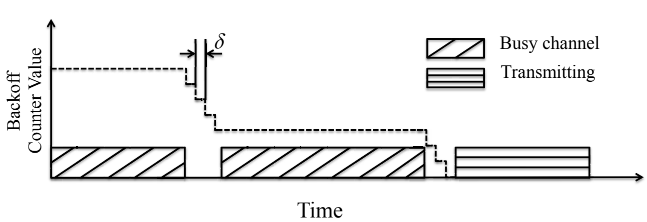

Figure 1: Back-off process in IEEE 802.11p.

- P is the transmit power, which is assumed to be the same for each node;
- $l(x, y)$ is the path loss or similar between x and y. Similar to [16], it is modeled as follows:
$$l(x, y) = A \min\left\{r_0^{-\alpha}, d(x, y)^{-\alpha}\right\},$$
where $d(x, y)$ is the Euclidean distance between x and y and α is the path loss exponent; we also use the path loss function in this form:
$$l(r) = A \min\left\{r_0^{-\alpha}, r^{-\alpha}\right\},$$
where $A = \left(\frac{\tilde{\lambda}}{4\pi r_0}\right)^{\alpha}$ is a dimensionless constant in the path loss law determined by the wavelength $\tilde{\lambda}$ and the reference distance r_0 for the antenna far field.
- S_y^x is a random variable denoting the fading between points x and y, and $\forall y$, the random variables $\left(S_y^{x_1}, S_y^{x_2}, \cdots\right)$ are assumed to be i.i.d. exponentially distributed with mean one, which means the channels are Rayleigh fading. For the non-fading case, $S_y^x \equiv 1$. In this paper, we consider both the fading and non-fading cases.

The neighborhood of a node x (denoted as $V(x)$) is defined as the random set of nodes in its contention domain, namely the set of nodes whose messages this node receives with a power larger than some detection threshold P_0, *i.e.*,

$$V(x) = \left\{y \in \Phi_{[W]} : P S_x^y l(y, x) > P_0\right\}, \quad x \in \Phi_{[W]}. \tag{2}$$

Equivalently,

$$V(x) = \left\{y \in \Phi_{[W]} : d(y, x) < R_x^y\right\}, \quad x \in \Phi_{[W]}. \tag{3}$$

where

$$R_x^y = \left(\frac{P A S_x^y}{P_0}\right)^{\frac{1}{\alpha}} \tag{4}$$

is called the carrier sensing range, which is a random variable related to S_x^y. In the non-fading case, $R = R_x^y = \left(\frac{PA}{P_0}\right)^{\frac{1}{\alpha}}$ is deterministic.

The impact of the vehicle mobility and direction is neglected since the node is almost stationary within one packet transmission duration, which is usually less than 1 ms.

III. Temporal Characteristics of V2V Communications

In this section, we will show that the vehicular networks dynamics can be explained using queueing theory.

A. Dense Networks

In [16], the authors claimed that when the network is dense that 1) after every busy period a node can decrease the value of its back-off counter only by one; 2) if almost all the sections of the road are covered by transmissions, the system performance under the CSMA-based protocol is similar to that of ALOHA. In other words, this means that the performance of such networks at high node density can be analyzed by approximating the slotted-CSMA network as a slotted-ALOHA network where the set of concurrently transmitting nodes Φ_{tx} forms a PPP. In [16], a slotted-CSMA

Notation	Description
$[W]$	$\{0, 1, \cdots, W\}$, the set of backoff counter values
Φ	Entire PPP of intensity λ_0
Φ^B	$\Phi \cap B, B \subset \mathbb{R}$. Nodes within B
$s_x(t)$	State (or mark) of node $x \in \Phi$ at time t
$\mathcal{S}$	A set of states of the nodes. $\mathcal{S} = [W] \cup \{\text{idle}\} \cup \{\text{tx}\}$. $i \in [W]$ is the state where the back-off counter is i and there is a packet waiting in the buffer to be transmitted. idle is the state where no packets are in the buffer. tx means that a packet is in transmission.
$\Phi_S(t)$	Subset of nodes with state $s(t) \in S \subset \mathcal{S}$.[5]
$\Phi_{i\downarrow}(t)$	Nodes that have a packet in the buffer and reduce the back-off counter to i from a different value by time t
$\Phi_{i\ddagger}(t)$	$\Phi_i(t) \backslash \Phi_{i\downarrow}(t)$, $i \in [W-1]$. Nodes with a packet in the buffer that select i as back-off counter value and have not decreased it by time t.
$\widehat{\Phi}_{\text{tx}}$	Set of concurrent transmitting nodes selected by Matern-II-discrete process
$\tilde{\Phi}_{\text{tx}}$	Set of concurrent transmitting nodes selected by Matern-II-continuous process

Table I: Notation

[5]E.g., $\Phi_{\text{tx}}(t)$ is the set of nodes that transmit at time t, $\Phi_3(t)$ is the set of nodes with back-off counter value 3 at time t, and $\Phi_{[W]}(t)$ is the set of nodes having a packet waiting to be transmitted at time t.

model is assumed to simplify the analysis. This assumption may introduce inaccuracies in the model but is an acceptable approximation in dense networks.

We analyze the distribution of Φ_{tx} by studying what happens after the transmissions of some nodes in Φ_{tx} finish. The assumption we make is that Φ_{idle} follows a PPP. If a subset of Φ_{tx} finish their transmissions at time $t\_$[4], they leave sections of the road (intervals of the real line) in which the channel is sensed idle. We pick any of the sections and call it s_1. Nodes in $\Phi_0^{s_1}(t)$ will start transmission immediately. Using queueing theory, we argue that $\Phi_0^{s_1}(t)$ forms a PPP. Define T_p as the transmission time of a packet followed by two slot times (as required by IEEE 802.11p). $\Phi_0^{s_1}(t) = \Phi_{0\downarrow}^{s_1}(t) \cup \Phi_{0\ddagger}^{s_1}(t)$. We claim that $\Phi_{0\ddagger}^{s_1}(t)$ forms a PPP on s_1 since the packet arrivals at each node are independent and $\Phi_{0\ddagger}^{s_1}(t)$ can be viewed as an independent thinning of $\Phi_{\text{idle}}((t-T_p)_+)$ where the thinning probability is the probability that a node has a packet arriving between $(t-T_p)_+$ and t and chooses its back-off counter to be 0. However, to understand the distribution of $\Phi_{0\downarrow}^{s_1}(t)$, we need to highlight that the back-off processes of the nodes in $\Phi_{[W]}^{s_1}$ are synchronized. In other words, they observe the same channel states (idle or busy) and start or stop back-off counters simultaneously.

Synchronization cannot generally be assumed across nodes in CSMA-based multi-hop networks due to hidden terminals. As a consequence, we need to understand how it occurs for nodes in $\Phi_{[W]}^{s_1}$. To do so, snapshots of the nodes' statuses are recorded in Fig. 2 on a section of the road at different times. Initially (as shown by the snapshot at T_0), we assume none of the nodes is transmitting. When the first packet arrives, it is transmitted without back-off process (since the channel is sensed idle). The following packets are held if their nodes are within the carrier sensing ranges of any ongoing transmissions. Nodes within the same carrier sensing range may synchronize the next transmission.

[4]We use $t\_$ to note the time just before t and t_+ for the time just after t

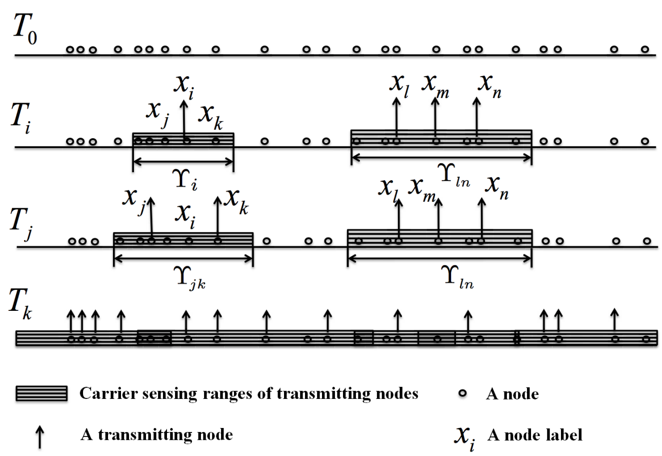

Figure 2: Snapshots of statuses of nodes on a section of road taken at four different times, T_0, T_i, T_j and T_k with $T_0 < T_i < T_j < T_k$ where Υ denotes the (union of) carrier sensing ranges of transmitting nodes.

Assume that x_j and x_k from the snapshot at T_i are two of those nodes and they are within the carrier sensing range of x_i (denoted as Υ_i). They both have their back-off counter values set to zero and start transmissions immediately after x_i finishes. The union of x_j's and x_k's carrier sensing ranges constitutes Υ_{jk} (shown in the snapshot at T_j). In this way, the region on which transmissions may be synchronized will increase from Υ_i to Υ_{jk}. The same process happens on other sections of the road, until almost the whole road is covered by transmissions (as shown by the snapshot at T_k).

The system now reaches a point where it can be viewed as a collection of regions on which nodes' back-off processes are synchronized and gaps between these synchronized regions. We can think of s_1 as any one of such regions where the back-off processes of nodes in $\Phi_{[W]}^{s_1}$ are synchronized. As a

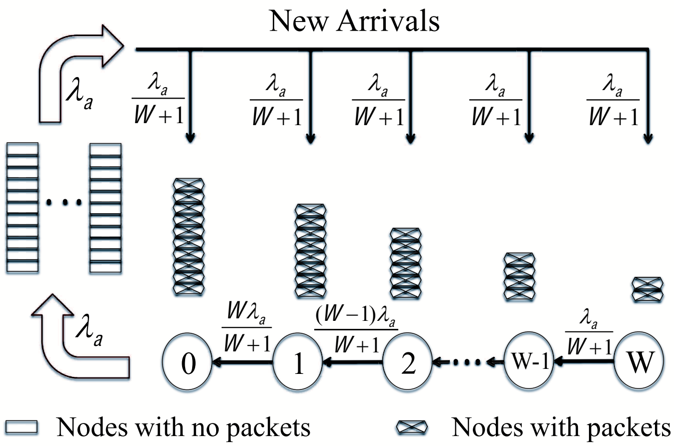

Figure 3: Markov chain model for the dense case where the nodes' back-off counter values are modeled as the states of the chain (from 0 to W) . The transition rates labeled between the states stand for the number of nodes per second per unit length of road that are able to change their back-off counter values.

consequence, $\Phi_{0\downarrow}^{s_1}(t)$ can be written as the union of $\Phi_{1\downarrow}^{s_1}(t - T_p)$ and $\Phi_{1\updownarrow}^{s_1}(t - T_p)$. Applying the same logic iteratively to $\Phi_{1\downarrow}^{s_1}(t - T_p)$ yields

$$\Phi_{0\downarrow}^{s_1}(t) = \bigcup_{i=1}^{W} \Phi_{i\updownarrow}^{s_1}(t - iT_p). \tag{5}$$

Since $\Phi_{i\updownarrow}^{s_1}(t - iT_p), i \in \{1, 2, \cdots, W\}$, are independent PPPs on s_1, $\Phi_{0\downarrow}^{s_1}(t)$, as the union of them, is also a PPP [13]. However, it does not mean Φ_{tx} follows a PPP on all the sections in the system which is assumed in [16]. Assume that after nodes in $\Phi_0^{s_1}(t)$ start transmitting, the transmitters in an adjacent region to s_1, named s_2, finish transmissions. Although $\Phi_0^{s_2}(t_2)$ forms a PPP where $t_2 > t$, there cannot be any transmitters in $s_1 \cap s_2$. In other words, there may be sections where the transmitters form a PPP, interleaved with sections without transmitters. Nevertheless, the transmitters in the dense case can be well approximated as a PPP as shown in the simulation later and [16].

The above process can be approximated using queueing theory where the counter values k for a given node can be considered as the states in a continuous-time Markov chain. As illustrated in Fig. 3, the density of nodes with new arriving packets can be considered as the mean arrival rate per unit length, and the density of transmitting nodes as the mean service rate per unit length. Assume that at steady state, the mean arrival rate per unit length (denoted as λ_a) is equal to the mean service rate per unit length (denoted as μ_a), that is, $\lambda_a = \mu_a$. The system acts as if the nodes have saturated data traffic, *i.e.*, the nodes finishing their transmissions will generate a new packet and join the queue that consists of the nodes with back-off counters immediately. Define q_{ki} as the transition rate at which the nodes make a transition from counter k to counter i. p_k represents the steady-state probability where the counter value is k. By the global balance equations for a continuous-time Markov chain [24], we have

$$p_k \sum_{i=0}^{W} q_{ki} = \sum_{i=0}^{W} p_i q_{ik}, \tag{6}$$

where the non-zero transition rates are $q_{k,k-1} = \lambda_a \left(1 - \frac{k}{W+1}\right)$ for $k \in [W]$ and $q_{0,k} = \frac{\lambda_a}{W+1}$ for $k \in [W]$ (their values labeled in Fig. 3). Therefore, for the dense case as in [16], we can compute the steady state probability p_k as

$$p_k = \frac{2\,(W - k)}{W\,(W + 1)} \tag{7}$$

using queueing theory, combining (6) and $\sum_{k=0}^{W} p_k = 1$. Expression (7) is equivalent to that in the one-hop communication networks in [5]. The difference is that a discrete-time Markov chain with variable slot assumption is used in [5] to obtain the steady state probability p_k while our continuous-time Markov chain model more naturally captures the steady state in any given time instant.

B. Sparse Networks

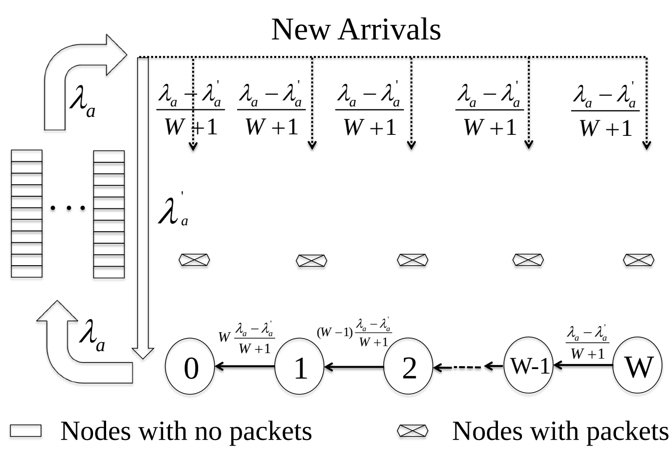

Figure 4: Markov chain model for the sparse case where the nodes' back-off counter values are modeled as the states of the chain (from 0 to W) . The transition rates labeled between the states stand for the number of nodes per second per unit length of the road that are able to change their back-off counter values.

Inspired by the work in [16], we explore the distribution of Φ_{tx} in sparse networks. According to IEEE 802.11p, a packet is transmitted immediately upon arrival if the channel is sensed idle. In sparse networks, a limited number of nodes exist. The cumulative channel load consumes only a small portion of the channel capacity, leaving the channel idle most of the time as observed in [25], which implies that most nodes will send out their packets without going through any back-off process (as indicated by λ_a' in Fig. 4). Furthermore, as there is a finite number of nodes within the same carrier sensing range and the packet arrival process is continuous, the probability that two nodes within the carrier sensing ranges of each other have packets arrive at exactly the same time is zero. Therefore, we will have no pairs of nodes within distance less than carrier sensing range that start transmissions at the same time, which can be modeled by the hard-core process described in [20]. However, beyond the space dependence introduced by the hard-core process, there is time dependence on the locations of transmitters. In fact, some nodes may have packets arrive when the channel is sensed busy, which may result in concurrent transmissions within the same carrier sensing range. This affects the accuracy of the hard-core process.

C. Networks with Intermediate Density

A relevant question is what the right model is for networks with intermediate densities. On the one hand, compared with sparse networks, more transmissions are delayed, increasing the probabilities of transmission collisions from synchronized back-off processes (but not as many as in dense networks). On the other hand, the transmissions may not cover almost all the sections of the road, leading to a distribution of transmitters different from the case of dense networks. For example, it could happen that on some sections of the road the channel is sensed idle but no nodes have packets and thus no transmissions take place. As a consequence, the distribution of the transmitters for intermediate networks cannot purely be modeled or approximated by hard-core processes or PPPs. Instead, it should be a hybrid process between hard-core and Poisson.

D. Observations

Based on the observations above, it is generally true that all the nodes with back-off counter at t_j have chances to participate in transmissions at t_i where $t_i > t_j$ if the channels turn idle before t_i. From a stochastic geometry perspective, the concurrent transmitters form a thinned process like the Matern-II-continuous process. However, to account for the concurrent transmitters within the same carrier sensing range, we need to discretize the marks in the Matern-II-continuous process, and any two nodes having the same mark should not silence each other. This discrete choice for the marks makes sense since the back-off counter in IEEE 802.11p takes integer values from 0 to W only and has concurrent transmissions if the counters of two nodes within each other's carrier sensing range hit zero simultaneously.

To obtain the non-uniform distribution from which marks are drawn, we sample the number of nodes having different back-off counter values from ns2 simulations. The empirical probability mass functions (PMFs) for scenarios with different densities λ_0 are shown in Fig. 5.

A few observations can be easily made from this plot. First, the PMF is not uniform. It is skewed towards small counter values. The maximally skewed curve is obtained from (7). Second, the empirical PMF for different densities can be approximated by an affine function of k. Assume that it follows the form

$$p_k = b - ak, \tag{8}$$

where $b \geq Wa \geq 0$. Since $\sum_{k=0}^{W} p_k = 1$, we have

$$p_k = \frac{1}{W+1} + \frac{W}{2}a - ak. \tag{9}$$

where $0 \leq a \leq \frac{2}{W(W+1)}$. a should be a function of the density λ_0. To obtain concrete results of $a(\lambda_0)$, we can estimate it from ns2 simulations or using queueing theory. Here, we proceed with the former method. In the following section, we will use it as the counter distribution or mark distribution for the Matern-II-discrete process.

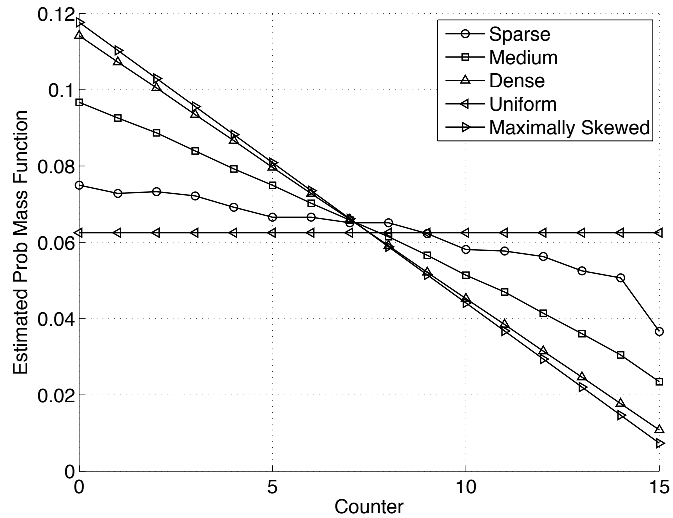

Figure 5: Estimated probability mass function of the nodes' back-off counter compared with the uniform PMF and maximally skewed PMF: node density $\lambda_0 = 0.033, 0.066, 0.132$ for the sparse, intermediate and dense cases, respectively.

IV. Matern-II-Discrete Process

Section III discussed the temporal characteristics of vehicular networks from a queueing theory perspective where the distribution of backoff counter is derived and the concurrently transmitting nodes are analyzed. Based on the analysis, we propose the Matern-II-discrete process to approximate the distribution of the concurrent transmitters of IEEE 802.11p in vehicular networks in this section.

A. Model Description

As mentioned in the system model, $\Phi_{[W]}$ is the set of nodes that have a packet waiting to be transmitted. Assume that it is a one-dimensional homogeneous PPP with density $\lambda < \lambda_0$, i.e., an independent thinning of Φ. Denote by $\widehat{\Phi}_{\text{tx}}$ the set of nodes selected by the CSMA-based broadcast protocol to transmit at a given time. $\widehat{\Phi}_{\text{tx}}$ is a dependent thinning of $\Phi_{[W]}$ built as follows: each point of $\Phi_{[W]}$ is attributed an independent mark which is discrete non-uniformly distributed in $[W]$. The discrete mark mimics the discrete back-off counter values. A point x of $\Phi_{[W]}$ is selected in the Matern-II-continuous process if its mark is smaller than or equal to that of any other point of $\Phi_{[W]}$ in its neighborhood $V(x)$. Hence, $\widehat{\Phi}_{\text{tx}}$ is defined by

$$\widehat{\Phi}_{\text{tx}} = \left\{ x \in \Phi_{[W]} : m(x) \leq m(y) \text{ for all } y \in V(x) \right\}, \tag{10}$$

where $m(x)$, denoting the mark of point x, models the back-off counter of the node and has the PMF given in (9), i.e., $\mathbb{P}\left(m(x) = k\right) = p_k$.

This model captures the fact that CSMA will grant a transmission opportunity to a given node if this node has the minimal back-off counter among all the nodes in its carrier sensing range and the fact that a node will be kept from transmitting if another node in its carrier sensing range already transmits. This is similar to the Matern-II-continuous process. The difference is that the marks have a discrete and non-uniform distribution instead of a continuous and uniform distribution, and hence this model can also include the concurrent transmissions since the probability of two nodes with the same mark is not equal to zero, *i.e.,* $\mathbb{P}\left(m(x)=m(y)\right)\neq 0$. This is a more accurate assumption in IEEE 802.11p for V2V communications as discussed in Section III-C.

B. Retaining Probability

Let $p^*=\mathbb{P}^0\left\{0\in\widehat{\Phi}_{\rm tx}\right\}$ be the Palm probability of retaining the typical point of $\Phi_{[W]}$ in the thinning defining $\widehat{\Phi}_{\rm tx}$. p^* can be rewritten as

$$p^*=\sum_{k=0}^{W}\mathbb{P}^x\left(x\in\widehat{\Phi}_{\rm tx}\mid m(x)=k\right)p_k. \tag{11}$$

Similar to the argument in [20], the following theorem can be obtained:

Theorem 1. *Given the probability mass function p_k of the back-off counter and Rayleigh fading, the probability for a typical node to be retained in the thinning from $\Phi_{[W]}$ to $\widehat{\Phi}_{\rm tx}$ is*

$$p^*=\sum_{k=0}^{W}\exp\left(-\lambda F_X\left(k\right)c\right)p_k \tag{12}$$

with

$$F_X(k)=\begin{cases}\sum_{i=0}^{k-1}p_i, & \text{if } k>0\\ 0, & \text{if } k=0.\end{cases} \tag{13}$$

$$c=2\pi\int_0^{+\infty}e^{-K\max(r_0,r)^\alpha}rdr, \tag{14}$$

where $K=P_0/PA$. For $\alpha=2$, $c=\pi e^{-Kr_0^2}\left(\frac{1}{K}+r_0^2\right)$.

The proof is omitted since it is similar to the case with uniform and continuous counter in [20]. The following corollaries give the retaining probability for the two special cases of the back-off counter distribution. One is the uniform discrete distribution corresponding to the sparse case, and the other the discrete distribution corresponding to the dense case.

Corollary 1. *For $p_k=\frac{1}{W+1}$, the retaining probability is*

$$\underline{p}=\frac{1}{W+1}\cdot\frac{1-e^{-\lambda c}}{1-e^{-\lambda c/(W+1)}}, \tag{15}$$

where c is given in (14).

Proof: Insert $p_k=\frac{1}{W+1}$ into (12), and it is straightforward to obtain the result. ■

As $\lambda\to 0$, $\underline{p}\to 1$, which means all nodes will transmit with probability one if the system is extremely sparse. Also, note that as $W\to\infty$, $\underline{p}\to\frac{1-e^{-\lambda c}}{\lambda c}$, which is the probability for a node to be granted transmission in the Matern-II-continuous process [20]. Hence, our mark distribution assumption generalizes the uniform mark distribution.

Corollary 2. *For $p_k=\frac{2(W-k)}{W(W+1)}$, the retaining probability is*

$$\bar{p}=\sum_{k=0}^{W}\frac{2(W-k)}{W(W+1)}\exp\left(-\lambda c\frac{k\left(2W+1-k\right)}{W(W+1)}\right), \tag{16}$$

where c is given in (14).

Proof: Inserting $p_k=\frac{2(W-k)}{W(W+1)}$ into (12), we obtain (16). ■

As $\lambda\to\infty$, $\bar{p}\to\frac{2}{W+1}$, which is the probability of the back-off counter to be zero. It means that when the system is extremely dense, only the nodes with back-off counter zero have a chance of transmitting. This is intuitive. From Theorem 1 and Corollaries 1 and 2, it is easy to see that the retaining probability is lower bounded by $\underline{p}$ and upper bounded by $\bar{p}$.

V. Performance Evaluation

Based on the newly proposed Matern-II-discrete process, we can evaluate the performance metric of interest for vehicular networks. It is well accepted that a packetized transmission is considered successful if the signal-to-interference-plus-noise ratio (SINR) is greater than some threshold [13]. So we define the transmission success probability as follows.

Definition 1. *The transmission success probability is the probability of successful transmission from node x to node y at distance $r=\|x-y\|$,*

$$p\left(r,T,\alpha\right)\triangleq\mathbb{P}\left(\mathit{SINR}\geq T\right), \tag{17}$$

where $\mathit{SINR}=\frac{P\cdot S_y^x(r)\cdot l(r)}{I(y)+N}$, $I(y)$ is the interference at the receiver y, and N is the noise power.

It is one of the most important metrics in evaluating the performance of vehicular networks. We will analyze the transmission success probability for ALOHA and CSMA and compare the transmission success probabilities for different models in the next subsection.

A. Transmission Success Probability for ALOHA

First, we define the thinning probability in the ALOHA MAC scheme. At any given time, the probability that a node is transmitting can be computed as $p=T_p/\tau$, where $\tau=0.1$ s is the packet generation period.

For comparison, the transmission success probability of ALOHA is given by the following theorem:

Theorem 2. *The transmission success probability with path loss exponent $\alpha=2$ and distance r is*

$$p\left(r,T,2\right)=\exp\left(-\lambda_0 p\sqrt{\pi T}r\right)\exp\left(-NTr^2/PA\right) \tag{18}$$

in the Rayleigh fading case, and it is

$$p(r,T,2)=1-\operatorname{erf}\left(\frac{\lambda_0 p\sqrt{\pi}}{\sqrt{1/Tr^2-N/PA}}\right) \tag{19}$$

in the non-fading case.

Proof. (18) is directly from [16]. For the non-fading case, the probability density function of the interference is [16]

$$f_I(y) = \frac{\lambda_0 p}{\sqrt{1/PA}} y^{-\frac{3}{2}} e^{-\frac{\lambda_0^2 p^2 \pi PA}{y}}. \tag{20}$$

Since

$$\int_0^a f_I(y)\, dy = 1 - \text{erf}\left(\frac{\lambda_0 p \pi^{\frac{1}{2}}}{\sqrt{a/PA}}\right), \tag{21}$$

it follows that

$$\begin{aligned} p(r,T,2) &= \mathbb{P}\left(\frac{PA}{r^2} \geq T(I+N)\right) && (22) \\ &= 1 - \text{erf}\left(\frac{\lambda_0 p \sqrt{\pi}}{\sqrt{1/Tr^2 - N/PA}}\right). && (23) \end{aligned}$$

□

B. Transmission Success Probability for CSMA

Since it is difficult to derive the transmission success probability for the Matern-II-discrete process model theoretically, an estimator similar to that in [20] is used to estimate the transmission success probability of the new model. First, the locations of the nodes with packets are sampled according to a PPP on the interval $[0, L]$. The density of this PPP is determined by the density of nodes with back-off counter at any given time instant, which include those from the previous time and the new arrivals. The power fading coefficient from each transmitting node to any other location is exponential with mean one (Rayleigh fading). The interference is evaluated as the sum of the powers of all other concurrent transmitting nodes. The Matern-II-discrete process $\widehat{\Phi}_{\text{tx}}$ with discrete and non-uniform counter is simulated using (10). To get rid of the border effect, the interval $[0, L]$ is considered as circular. The counter distribution is given by (9) with slope a estimated from simulation data.

The transmission success probability is calculated using the estimator

$$\hat{p}_a(r,T,2) = \frac{1}{2}\mathbb{E}\left[\frac{\sum_{x\in\widehat{\Phi}_{\text{tx}}^{[0,L]}}\left[\mathbb{1}_B + \mathbb{1}_C\right]}{\left|\widehat{\Phi}_{\text{tx}}^{[0,L]}\right|} \mid \widehat{\Phi}_{\text{tx}}^{[0,L]} \neq \emptyset\right], \tag{24}$$

where $B = \left\{\frac{PAS^x_{x+r} r^{-2}}{I(x+r)+N} \geq T\right\}$ and $C = \left\{\frac{PAS^x_{x-r} r^{-2}}{I(x-r)+N} \geq T\right\}$. B (or C) is the event that for a given node $x \in \widehat{\Phi}_{\text{tx}}$ the SINR at distance r right (or left) from x is greater than or equal to the threshold T. $\left|\widehat{\Phi}_{\text{tx}}^{[0,L]}\right|$ indicates the number of nodes in $\widehat{\Phi}_{\text{tx}}$ in the interval $[0, L]$.

The Matern-II-continuous process is formed by dependent thinning with the following definition

$$\tilde{\Phi}_{\text{tx}} = \left\{x \in \Phi_{[W]} : m_b(x) < m_b(y) \text{ for all } y \in V(x)\right\}, \tag{25}$$

where $m_b(x)$ is the mark of $x \in \Phi_{[W]}$, which is uniformly distributed on $[0, 1]$ [20]. The estimator of the transmission success probability of the Matern-II-continuous process is given in a similar way:

$$\hat{p}_b(r,T,2) = \frac{1}{2}\mathbb{E}\left[\frac{\sum_{x\in\tilde{\Phi}_{\text{tx}}^{[0,L]}}\left[\mathbb{1}_B + \mathbb{1}_C\right]}{\left|\tilde{\Phi}_{\text{tx}}^{[0,L]}\right|} \mid \tilde{\Phi}_{\text{tx}}^{[0,L]} \neq \emptyset\right]. \tag{26}$$

C. Performance Comparison

We compare the transmission success probabilities for ALOHA, Matern-II-discrete process and Matern-II-continuous process, while using simulations from ns2 as the baseline. ns2 has been widely accepted by the research community due to its capability to accurately simulate communications in a large variety of wireless environments. For vehicle-to-vehicle broadcast service in highway scenarios, the articles [1], [21] describe work carried out to further improve the realism of simulations and a large number of publications therefore used ns2 to provide ground truth data (e.g., [16]). In this paper, we rely on the ns2.34 simulator. We implemented the EDCA back-off process and calibrated it with work in [22]. We set up a circular road of $L = 10$ km and randomly place the nodes. The speed of the vehicles is ignored because they barely move in the transmission time of one single packet and only relative positions matter. All other simulation parameters are summarized in Table II.

Parameter	Value
carrier frequency	5.9 GHz
packet size	414 Byte
noise floor	-99 dBm
transmit power	10 dBm
broadcasting contention window $(W+1)$	16
periodicity	100 ms
slot time δ	$13\mu s$
modulation	BPSK
broadcast rate	6 Mbps
path loss exponent α	2
path loss constant A	-17.86 dBm
reference distance r_0	1
SINR threshold T	7 dB
simulation length L	10 km

Table II: Simulation Parameters

Fig. 6 shows the transmission success probabilities of the various models for the non-fading case under different node densities λ_0. Fig. 6(a) validates that the concurrent transmitters in IEEE 802.11p form a hard-core process in the sparse case as discussed in Section III-B. For the near distance (less than 300 m), the transmission success probability of the ns2 simulations is very close to that of two Matern type II models. There is little difference between the Matern-II-continuous and Matern-II-discrete processes since the probability that nodes within each other's carrier sensing range are transmitting simultaneously is zero in the sparse case.

For the intermediate-density case, the Matern-II-discrete process produces a lower transmission success probability than the Matern-II-continuous process as it allows for nodes to have the same marks. Although none of the three models can match ns2 simulations very well due to the complexity of networks with intermediate densities, the Matern-II-discrete process provides the closest approximation within 100-200 m, which is the most critical range to vehicular safety [2], [26], [27].

In the dense case, the Matern-II-discrete process matches the ns2 simulation precisely. The transmission success probability for ALOHA is also close to that of the ns2 simulation in the dense case as claimed in [16] while it seems to be a very loose lower bound for the sparse and intermediate cases. The transmission success probability for the Matern-II-continuous process for the intermediate and dense cases look alike because there is saturation phenomenon in its intensity λ_b, *i.e.*, λ_b is upper bounded by $\lambda_{b,\max} = \frac{1}{2R}$, where R is the carrier sensing range in (4). For the non-fading case, R is fixed, and hence the maximum average number of retained nodes on a road of length L from the Matern-II-continuous process is upper bounded by $\frac{L}{2R}$, which is independent of λ.

For the fading case, the performance of the Matern-II-discrete process shows the same trend as in the non-fading case. However, ALOHA seems to have good performance as well. This can be explained by the fact that fading randomizes the interference and therefore the actual network is perceived as an equivalent Poisson network. A similar observation was made in [28] in the case of cellular networks. In other words, fading dampens the hard-core effect and makes the transmitter distribution look more like a PPP to the receivers. In addition, the lack of RTS/CTS may further reduce the hard-core effect.

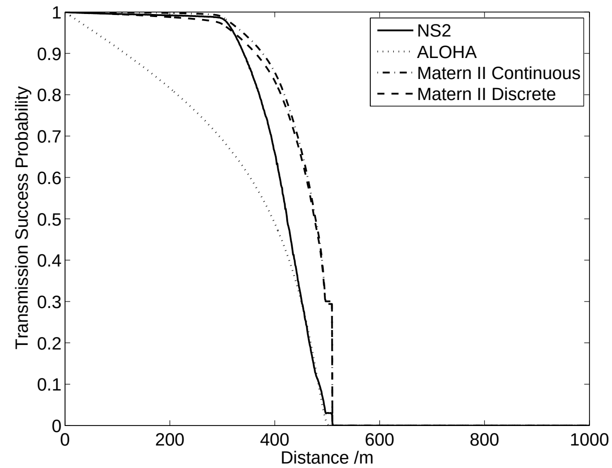

(a) Sparse case with density $\lambda_0 = 0.033$

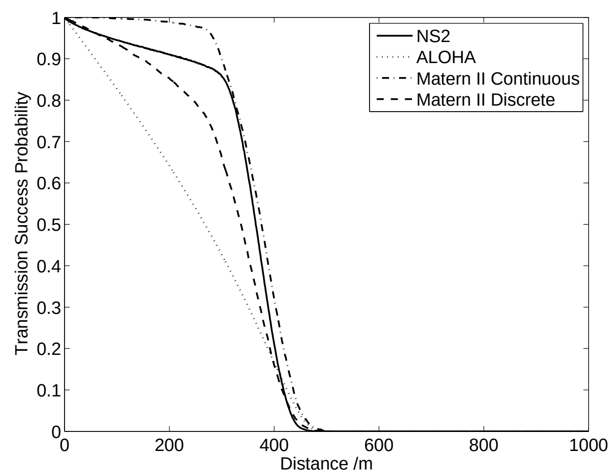

(b) Intermediate-density case with density $\lambda_0 = 0.066$

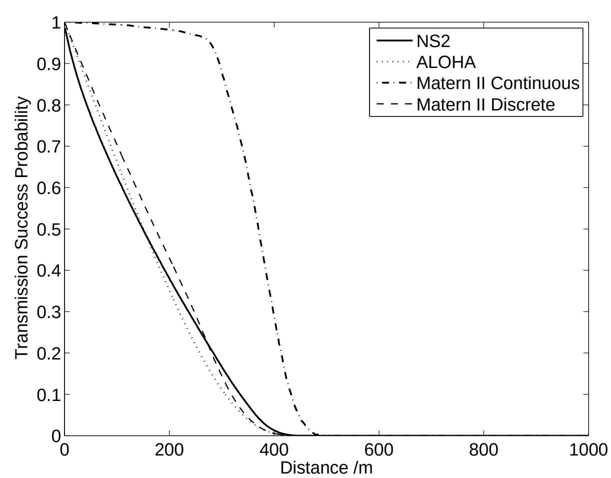

(c) Dense case with density $\lambda_0 = 0.132$

Figure 6: Transmission success probability of different models for the non-fading case: the transmission success probabilities for the two Matern type II processes are averaged over 10^4 realizations.

VI. Conclusions

In this paper, we explored the geometric modeling of DSRC for V2V safety communications by using tools from stochastic geometry and queueing theory. Firstly, we analyzed the distribution of transmitters for networks with different densities. We found that without considering fading, by increasing the network density, the transmitter distribution changes from a hard-core model to a PPP model. With fading, the randomness of interference increases, which makes the networks appear as an equivalent Poisson network. In other words, the transmitters behave like a PPP from the receivers' perspective. Secondly, we proposed to use a non-uniform discrete distribution to replace the uniform distribution for the marks in the Matern-II-continuous process. The resulting Matern-II-discrete process therefore retains concurrent transmitters within the same carrier sensing range and thus approximates the network dynamics more precisely than the Matern-II-continuous process. Thirdly, we compared our models with simulations from ns2. The results show that our model performs well in a wide range of network densities.

References

[1] Q. Chen, F. Schmidt-Eisenlohr, D. Jiang, M. Torrent-Moreno, L. Delgrossi, and H. Hartenstein, "Overhaul of IEEE 802.11 modeling and simulation in ns-2," in *the 10th International Symposium on Modeling Analysis and Simulation of Wireless and Mobile Systems, MSWiM 2007, Chania, Crete Island, Greece, October 22–26, 2007*. ACM, 2007, pp. 159–168.

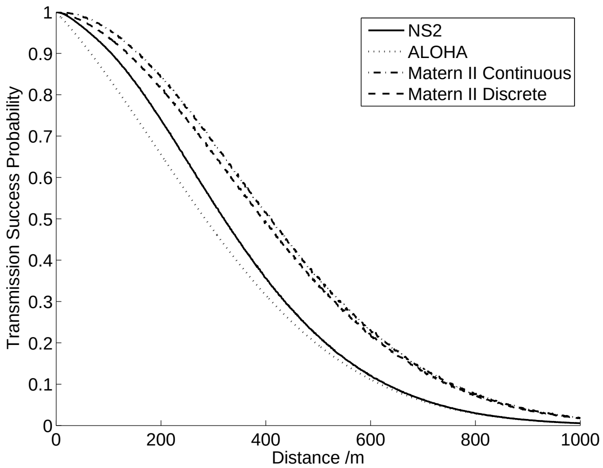

(a) Sparse case with density $\lambda_0 = 0.033$

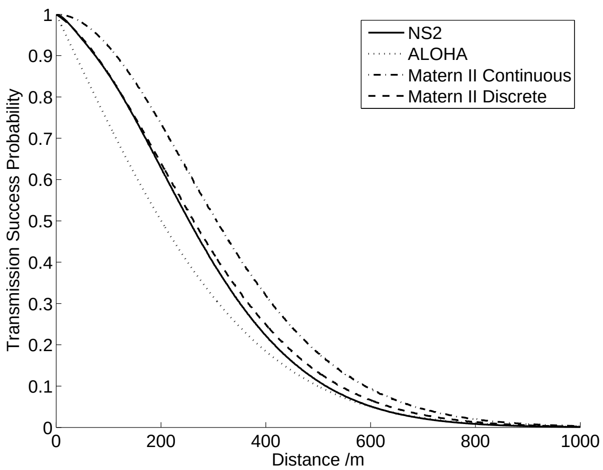

(b) Intermediate-density case with density $\lambda_0 = 0.066$

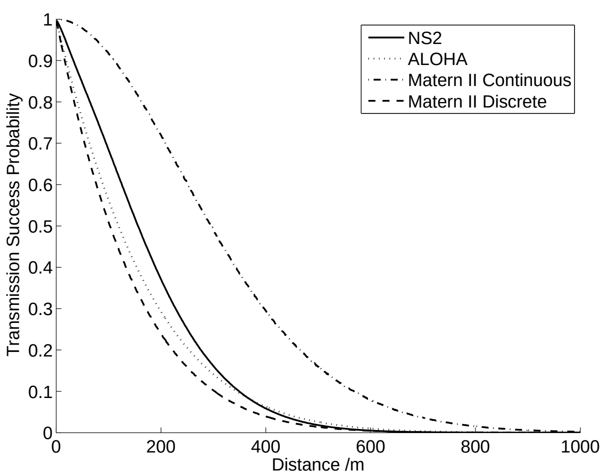

(c) Dense case with density $\lambda_0 = 0.132$

Figure 7: Transmission success probability of different models for the fading case: the transmission success probabilities for the two Matern type II processes are averaged over 10^5 realizations.

[2] M. Torrent-Moreno, J. Mittag, P. Santi, and H. Hartenstein, "Vehicle-to-vehicle communication: Fair transmit power control for safety-critical information," *IEEE Transactions on Vehicular Technology*, vol. 58, no. 7, pp. 3684–3703, Sept. 2009.

[3] D. Tse and P. Viswanath, *Fundamentals of Wireless Communications*. Cambridge University Press, 2005.

[4] G. Bianchi, "Performance analysis of the IEEE 802.11 distributed coordination function," *IEEE Journal on Selected Areas in Communications*, vol. 18, no. 3, pp. 535–547, March 2000.

[5] G. Bianchi, L. Fratta, and M. Oliveri, "Performance evaluation and enhancement of the CSMA/CA MAC protocol for 802.11 wireless LANs," in *Seventh IEEE International Symposium on Personal, Indoor and Mobile Radio Communications, PIMRC'96*, vol. 2, Oct 1996, pp. 392–396.

[6] F. Daneshgaran, M. Laddomada, F. Mesiti, and M. Mondin, "Unsaturated throughput analysis of IEEE 802.11 in presence of non ideal transmission channel and capture effects," *IEEE Transactions on Wireless Communications*, vol. 7, no. 4, pp. 1276–1286, April 2008.

[7] Y. Fallah, C. L. Huang, R. SenGupta, and H. Krishnan, "Analysis of information dissemination in vehicular ad-hoc networks with application to cooperative vehicle safety systems," *IEEE Transactions on Vehicular Technology*, vol. 60, no. 1, pp. 233–247, Jan. 2011.

[8] A. Tsertou and D. Laurenson, "Revisiting the hidden terminal problem in a CSMA/CA wireless network," *IEEE Transactions on Mobile Computing*, vol. 7, no. 7, pp. 817–831, July 2008.

[9] C. Han, M. Dianati, R. Tafazolli, R. Kernchen, and X. Shen, "Analytical study of the IEEE 802.11p MAC sublayer in vehicular networks," *IEEE Transactions on Intelligent Transportation Systems*, vol. 13, no. 2, pp. 873–886, 2012.

[10] Y. Yao, L. Rao, and X. Liu, "Performance and reliability analysis of IEEE 802.11p safety communication in a highway environment," *IEEE Transactions on Vehicular Technology*, vol. 62, no. 9, pp. 4198–4212, 2013.

[11] F. Baccelli and B. Blaszczyszyn, "Stochastic Geometry and Wireless Networks, Volume II - Applications," *Found. Trends Netw.*, vol. 2, no. 1-2, pp. 1–312, 2009.

[12] Z. Tong and M. Haenggi, "Throughput analysis for wireless networks with full-duplex radios," in *Wireless Communications and Networking Conference (WCNC), 2015 IEEE*, New Orleans, L, March 2015, pp. 717–722.

[13] M. Haenggi, *Stochastic Geometry for Wireless Networks*. Cambridge University Press, 2012.

[14] Z. Tong and M. Haenggi, "A Throughput-Optimum Adaptive ALOHA MAC Scheme for Full-Duplex Wireless Networks," in *2015 IEEE Global Communications Conference (GLOBECOM'15)*, San Diego, CA, Dec. 2015, accepted.

[15] ——, "Throughput analysis for full-duplex wireless networks with imperfect self-interference cancellation," *IEEE Transactions on Communications*, vol. 63, no. 11, pp. 4490–4500, Nov 2015.

[16] T. V. Nguyen, F. Baccelli, K. Zhu, S. Subramanian, and X. Z. Wu, "A performance analysis of CSMA based broadcast protocol in VANETs," in *2013 IEEE INFOCOM*, 2013, pp. 2805–2813.

[17] B. Błaszczyszyn, P. Muhlethaler, and Y. Toor, "Maximizing throughput of linear Vehicular Ad-hoc NETworks (VANETs) – a stochastic approach," in *2009 European Wireless Conference*, 2009, pp. 32–36.

[18] ——, "Stochastic analysis of Aloha in vehicular ad hoc networks," *Annals of Telecommunications*, vol. 68, no. 1-2, pp. 95–106, 2013. [Online]. Available: http://dx.doi.org/10.1007/s12243-012-0302-2

[19] D. H. Thuan, H. V. Cuu, and H. N. Do, "VANET modelling and statistical properties of connectivity in urban environment," *REV Journal on Electronics and Communications*, vol. 3, no. 1-2, January–June 2013.

[20] H. Nguyen, F. Baccelli, and D. Kofman, "A stochastic geometry analysis of dense IEEE 802.11 networks," in *2007 IEEE INFOCOM*, May 2007, pp. 1199–1207.

[21] J. Kunisch and J. Pamp, "Wideband car-to-car radio channel measurements and model at 5.9 GHz," in *Vehicular Technology Conference, 2008. VTC 2008-Fall. IEEE 68th*, Sept 2008, pp. 1–5.

[22] *Vehicle Safety Communications - Applications (VSC-A) Final Report*. National Highway Traffic Safety Administration, 2011.

[23] X. Shen, X. Cheng, R. Zhang, B. Jiao, and Y. Yang, "Distributed congestion control approaches for the IEEE 802.11p vehicular networks," *IEEE Intelligent Transportation Systems Magazine*, vol. 5, no. 4, pp. 50–61, winter 2013.

[24] D. Bertsekas, R. Gallager, and P. Humblet, *Data networks*. Prentice-Hall International, 1992.

[25] G. Bansal, J. Kenney, and A. Weinfield, "Cross-validation of DSRC radio testbed and ns-2 simulation platform for vehicular safety communications," in *2011 IEEE Vehicular Technology Conference (VTC Fall)*, 2011, pp. 1–5.

[26] *Vehicle Safety Communications-Applications (VSC-A) Final Report: Appendix Volume 1*. National Highway Traffic Safety Administration, 2011.

[27] X. Cheng, L. Yang, and X. Shen, "D2D for intelligent transportation systems: A feasibility study," *IEEE Transactions on Intelligent Transportation Systems*, vol. PP, no. 99, pp. 1–10, 2015.

[28] B. Błaszczyszyn, M. Karray, and H. Keeler, "Using Poisson processes to model lattice cellular networks," in *2013 IEEE INFOCOM*, 2013, pp. 773–781.

Zhen Tong received the B.Eng. degree in automation from Harbin Institute of Technology, China, in 2009, and the M.S. and Ph.D. degrees in electrical engineering from the University of Notre Dame, Notre Dame, IN, USA, in 2012 and 2015, respectively. He is currently a Senior Engineer at Qualcomm Technologies Inc., San Diego, CA, USA, where he works on modem software design and development. His research interests include power control and energy efficient MAC design, and analysis and implementation of full-duplex wireless networks.

Hongsheng Lu received the B.S. and M.S. in Electrical Engineering from Beihang University, Beijing, China, in 2006 and 2009, respectively. He started working towards Ph.D. degree in Computer Science and Engineering from 2009 in University of Notre Dame, Notre Dame, IN. His interests are congestion control in DSRC-based vehicle-to-vehicle safety communications.

Martin Haenggi (S'95, M'99, SM'04, F'14) is a Professor of Electrical Engineering and a Concurrent Professor of Applied and Computational Mathematics and Statistics at the University of Notre Dame, Indiana, USA. He received the Dipl.-Ing. (M.Sc.) and Dr.sc.techn. (Ph.D.) degrees in electrical engineering from the Swiss Federal Institute of Technology in Zurich (ETH) in 1995 and 1999, respectively. For both his M.Sc. and Ph.D. theses, he was awarded the ETH medal, and he received a CAREER award from the U.S. National Science Foundation in 2005 and the 2010 IEEE Communications Society Best Tutorial Paper award. He served as an Associate Editor for five journals from 2005-2013 and presently is the chair of the Executive Editorial Committee of the IEEE Transactions on Wireless Communications. He also was a Distinguished Lecturer for the IEEE Circuits and Systems Society in 2005-2006, a TPC Co-chair of the Communication Theory Symposium of the 2012 IEEE International Conference on Communications (ICC'12) and of the 2014 International Conference on Wireless Communications and Signal Processing (WCSP'14), a General Co-chair of the 2009 International Workshop on Spatial Stochastic Models for Wireless Networks (SpaSWiN'09) and the 2012 DIMACS Workshop on Connectivity and Resilience of Large-Scale Networks, and a Keynote Speaker of SpaSWiN'13, WCSP'14, and the 2014 IEEE Workshop on Heterogeneous and Small Cell Networks. He is a co-author of the monograph "Interference in Large Wireless Networks" (NOW Publishers, 2009) and the author of the textbook "Stochastic Geometry for Wireless Networks" (Cambridge University Press, 2012). His scientific interests include networking and wireless communications, with an emphasis on cellular, amorphous, ad hoc, cognitive, and, sensor networks.

Christian Poellabauer (S'97, M'04, SM'09) received his degree of Diplom Ingenieur in Computer Science from the Vienna University of Technology, Austria, in 1998 and his Ph.D. degree in Computer Science from the Georgia Institute of Technology, Atlanta, GA, in 2004. He is currently an Associate Professor in the Department of Computer Science and Engineering at the University of Notre Dame. His research interests are in the areas of wireless sensor networks, mobile computing, ad-hoc networks, pervasive computing, and mobile healthcare systems. He has published more than 90 papers in these areas and he has co-authored a textbook on Wireless Sensor Networks. His research has received funding through the National Science Foundation (including a CAREER award in 2006), National Institutes of Health, Army Research Office, Office of Naval Research, IBM, Intel, Toyota, GE Health, the National Football League, Serim Research Corporation, and Motorola Labs.